Original article

Upgrading the preparation of high-quality chitosan from *Procambarus clarkii* wastes over the traditional isolation of shrimp chitosan

Belal A. Omar [a], Ragab Elmasry [a], Ahmed Eita [a], Mohamed Mohamed Soliman [b], Amira M. El-Tahan [c], Mahmoud Sitohy [a,*]

[a] Biochemistry Department, Faculty of Agriculture, Zagazig University, 44519, Egypt
[b] Clinical Laboratory Sciences Department, Turabah University College, Taif University, 21995, Saudi Arabia
[c] Plant Production Department, Arid Lands Cultivation Research Institute, The City of Scientific Research and Technological Applications, SRTA-City, Borg El Arab, Alexandria, Egypt

ABSTRACT

Crustacean waste is one of the most severe issues, posing significant environmental and health risks. This study aims to improve managing marine waste by isolating chitosan from *Procambarus clarkii* by devising a new methodology, incorporating technical steps, e.g., washing, decolorization and deacetylation under a reflexive condenser and dialysis purification. A comparison was made between the prepared *P. clarkii* chitosan and four types of shrimp chitosans: commercial, high, low, and nano. The obtained chitosan has a low molecular weight and viscosity compared to the commercial shrimp chitosan used in various applications. *P. clarkii* chitosan was prepared in high quality from a cheap source, as its color and quality were better than those of the commercial shrimp chitosan. The new methodology has successfully extracted chitosan from *P. clarkii* in a good quality and high purity, achieving 89% deacetylation, high solubility, high purity, and medium molecular weight. Analysis of the different chitosan samples with Fourier transform infrared spectroscopy (FTIR), atomic force microscopy, Raman spectrum referred indicated high similarity between the chitosan different types, regardless of its source. The 3D image of *P. clarkii* showed the distance between the highest and most profound points of extracted chitosan is 728.94 nm, revealing homogeneous, smooth surfaces, apparently free of pores and cracks. FTIR and Raman spectrum of *P. clarkii* indicated various functional groups, e.g., alcohol, amines, amides, and phenols. These active groups are responsible for about 60% of the antioxidant activity of that product. Evaluating the quality traits indicated the excellence of the chitosan prepared from *P. clarkii*, especially in color, viscosity, and antioxidant activity, nominating it for different food applications.

© 2021 The Author(s). Published by Elsevier B.V. on behalf of King Saud University. This is an open access article under the CC BY-NC-ND license (http://creativecommons.org/licenses/by-nc-nd/4.0/).

1. Introduction

Red swamp crayfish (*Procambarus clarkia*) poses many problems, as a heavy eater of tilapia and Nile fish. *P. clarkii badly* affected soils, crops, and the environment. It is a vector for the fungus *Aphanomycesastaci*. The use of *P. clarkii* as a source of chitosan may convert its threats into useful applications. Preparing chitosan has many approaches but the method giving the best physical and chemical characterization regarding size and surface morphology is still lacking. Chitosan is gaining popularity because it meets environmental standards, such as being an eco-friendly compound that aids in the efficient use of reagents while reducing potential wastes (El-Naggar et al., 2021). Chitosan is a natural cationic biopolymer and is considered the second most abundant polymer after cellulose (Aranaz et al., 2009). Due to its amino groups' protonation, chitosan is soluble in dilute solutions of some organic acids at (pH 6), and it can interact with polyanions to form polyelectrolyte complexes because of its polycationic nature (Peniche and Argüelles-Monal, 2001). The cationic character of chitosan might impart it with valuable antiviral or antibacterial activities in a manner similar to cationic proteins, previously reported having antibacterial (Sitohy et al. 2011, 2012, 2013; Abdel-Shafi et al., 2016; Osman et al., 2016) and antiviral activities (Abdelbacki et al., 2010; Chobert et al., 2007; Swelum et al., 2020; Taha et al. 2010, Sitohy et al. 2006, 2007, 2020, 2021a,b).

Chitosan is obtained by deacetylating chitin, which is the second most abundant biopolymer after cellulose and is available in many insects' exoskeletons, the cell walls of many fungi, and the shells of crustaceans. It's also found in landfills from processing marine foods like shrimp, crab, and krill shells (Simpson et al., 1994). Chitosan has beneficial properties, high solubility, biocompatibility, biodegradability, and immune-restorative properties while exerting no toxicity (Shard et al., 2014). Chitosan can be modified, thus allowing different uses in various fields, including aquaculture, agriculture, cancer therapy, other medical fields, cosmetics, textiles, water treatment, and biochemical engineering (Zhao et al., 2018). The relationship between chitosan molecular weight and its water solubility follows a similar pattern to molecular weight and biological activities: the lower the molecular weight, the greater the solubility of the carbohydrate molecule (Pillai et al., 2009).

Red swamp crayfish (*Procambarus clarkia*) is a freshwater compared lobster, native to Mexico and the United States that settled in Egypt in the 1990s. Because of their higher chitin and lower protein content, the wastes of the crayfish *P. clarkii* are considered excellent sources of chitin. Their wastes contain 23.5% chitin, compared to 13–15% chitin by weight in shrimp wastes and 14–27% in crab wastes, respectively (No and Meyers, 1989). Recycling shell wastes and extracting commercially viable substances like chitin from them is a fast and effective solution. Chitin has various uses on its native status and can be deacetylated to produce chitosan, which has various applications (Kumar, 2000).

Furthermore, the crayfish industry in Egypt has expanded in the last five years, and the major issue facing crayfish plants is how to dispose of their solid wastes, which may accumulate to hundreds of tones, since the inedible portion of the animal accounts only for 60–70% of the total body weight (Ibrahim and Khalil, 2009). Chitosan was extracted from the exoskeleton wastes of *P. clarkii* the derived chitosan powder was buff in color, compared to the white color of commercial chitosan extracted from shrimp exoskeleton wastes. (El-Naggar et al., 2019).

This study aims to produce high purity chitosan from the harmful wastes of *P. clarkii* through optimizing a new technique using different solvents, minimizing the use of chemicals, and improving the purification steps. FTIR, and Raman microscopy physicochemically characterized the prepared chitosan. In addition, DPPH assay estimated the antioxidant activity of the prepared chitosan.

2. Materials and methods

2.1. Preparation of shrimp chitosan

2.1.1. High molecular weight chitosan

Fig. 1 shows the traditional isolation method of High molecular weight shrimp chitosan (Divya et al., 2014) with some modifica-
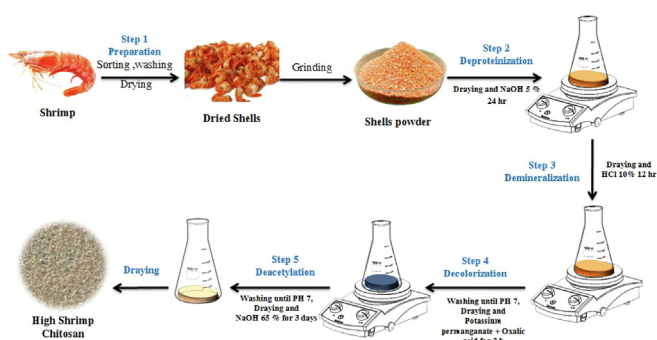
tions. First, an amount (100 g) of shrimp shell waste was treated with 5% NaOH at room temperature for 24 h to deproteinize the product, then washed with distilled water till the pH dropped to 7. Next, the deproteinized shells were treated with 5% HCl at room temperature for 12 h to liberate chitin, washed with distilled water, and dried at room temperature. The resulting chitin had a pink color. So, a decolorization step was achieved by soaking chitin soaking in 1% permanganate potassium and 1% oxalic acid for 3 h. Next, the decolorized chitin was deacetylated to chitosan by treating it with 65% NaOH for three days at room temperature. Finally, alkali was drained off, and the remaining material was repeatedly washed with distilled water till pH 7. Chitosan was further dried at 50 °C in an oven.

2.1.2. Low molecular weight chitosan

Chitosan was extracted from shrimp shells and converted into low molecular mass chitosan, according to (Kasaai et al., 2013). High molecular weight chitosan (1gm) was homogenized in 100 mL HCl (0.05 M) and stirred for 12 h at room temperature, then 100 mL of HCl (2.3 M) was added to obtain chitosan concentrate as 1.17 M HCl0.5%, w/v. The stirring continued for 30 h at 65 °C in a spherical flask. A portion of the resultant solution was cooled to 4 °C, and the other portion was kept at 25 °C. A different section was used to retrieve chitosan fragments. The fragments were used to determine intrinsic viscosity and characterize structural properties. The fragments were retrieved from chitosan suspension solutions following the fragmentation process by neutralizing the solution with NaOH (1.0 N), centrifugation, washing with deionized water, and lyophilization.

2.1.3. Nano-chitosan

Shrimp chitosan nanoparticles were prepared by the ionic gelation of tri-sodium polyphosphate (TPP) with chitosan following (Liu and Gao, 2009) with some modifications. First, 100 mL of chitosan solution (in 1% acetic acid) were dissolved in 20 mL of 0.1% TPP (in distilled water), then stirred at room temperature, centrifuged at 10,000 rpm for 10 min. Finally, the obtained precipitate was washed with ethanol, then distilled water and air-dried.

2.2. Isolation of P. clarkii chitosan

Chitosan isolation followed (Puvvada et al., 2012) with some modifications. The procedure comprised the following seven steps:

2.2.1. Preparation of shell powder

Shells of *P. clarkii* were obtained from the Royal Company for fish products (Alexandria - Egypt). The shells were thoroughly washed with water to remove impurities and protein residues. Fig. 2 shows the new method of isolation as follows. The shells were dried in an oven at 60 °C for 48 h before powdering to a homogenized product (<20 mesh).

2.2.2. Washing

A quantity (10 g) of P. clarkii shells powder was washed by distilled water to release any soluble impurities. This process is repeated several times until the disappearance of all the impurities. After that, the residue was kept in an oven at 80 °C until weight stabilization.

2.2.3. Demineralization

Dried *P. clarkii* shells powder were homogenized in 50 mL HCl (10%) (1:5, w/v). The reaction proceeded at room temperature on a magnetic stirrer at 200 rpm for 12 h. The demineralized shells were filtrated and washed with distilled water until reaching a neutral pH 7. The sample was dried in an oven at 80 °C until reaching a stable weight.
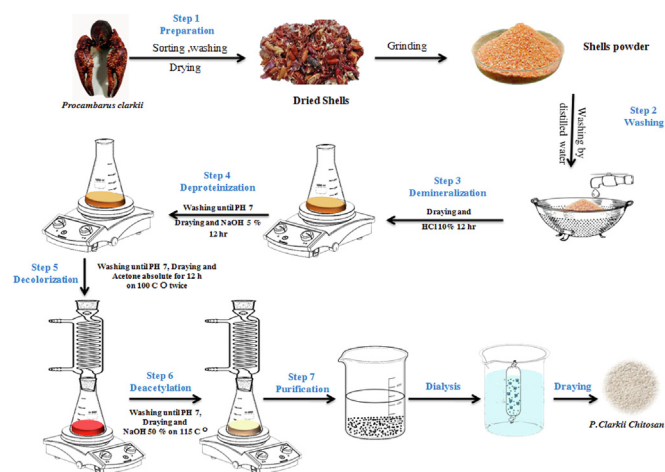

Fig. 1. Steps of Shrimp chitosan extracting.

Fig. 2. Steps of *P. clarkii* chitosan extracting.

2.2.4. Deproteinization

Protein was eliminated from the sample by adding 4–5% NaOH to the dried demineralized shells at a solid/liquid ratio of 1:10 (g/mL). The reaction slurry was blended on a magnetic stirrer at 200 rpm for 12 h. The insoluble solids were separated by filtration and washed with distilled water until reaching a neutral pH 7 before keeping in oven at 80 °C until a stable weight.

2.2.5. Decolorization

The dried deproteinized shell powder was immersed in acetone for 12 h at the boiling degree (70 °C), to remove the orange and red color. This step was conducted using a reflective condenser to bring back the evaporated acetone into the extracting vessel. The resulting chitin was dried in an oven at 80 °C until weight stabilization.

2.2.6. Deacetylation

The deacetylation of chitin was achieved by reacting the dried chitin with NaOH (45–50%) at a ratio of 1:10 (solid/liquid, g/mL). The reaction mixture was kept at 115C and agitated on a magnetic stirrer at 200 rpm for 24 h under a reflective condenser to maintain a constant mixture volume. The resulting insoluble product (chitosan) was filtrated, washed with distilled water until reaching a neutral pH 7. The washed product was dried in an oven at 70 °C until constant weight.

2.2.7. Purification

The chitosan was purified using the re-precipitation process, i.e., dissolving in acetic acid followed by precipitation with NaOH. The chitosan was dissolved in 3 percent (v/v) aqueous acetic acid overnight, and the resulting gel was filtered through a sintered glass funnel to extract undissolved and gelatinous particles after complete dissolution. Chitosan was precipitated by adding 1 M aqueous NaOH solution drop by drop while stirring. Finally, the regenerated chitosan was washed with distilled water until it was neutral, vacuum dried, and ground into a fine powder in a laboratory agate mortar. The final product was dispersed in distilled water and dialyzed against distilled water for two days at 5 °C.

2.3. Physicochemical characterization of chitosan

2.3.1. Solubility

One gram of the tested chitosans was dispersed in acetic acid solution 1% and mixed on magnetic stirred at 80 °C for 20 min. Then dispersion was centrifuged at 5000 rpm for 5 min undercool-

ing. The sediment was separated, lyophilized, weighed. The weight of the sediment is subtracted from the total weight. Solubility was calculated according to the following equation:

$$Solubility = \frac{Total\ weight - Residual\ weight}{Total\ weight} \times 100$$

2.4. Molecular weight

Chitosan molecular weight was derived from the viscosity value according the following equation (Czechowska-Biskup et al., 2018).

$$\eta = KM^{\alpha}$$

Relative viscosity was estimated for the four types of shrimp chitosan (High, low, Nano Shrimp) and *P. clarkii* chitosan, by Ostwalld Viscometer (MVMO4; Mayland instrument, India).

2.4.1. Fourier transform infrared spectroscopy (FTIR)

FTIR (Fourier-transform infrared) spectroscopy was carried out at the Central Laboratory of the Faculty of Science, Ain Shams University. FTIR spectra of chitosan were obtained using an FTIR 4100 (Jasco, Japan) spectrophotometer. The scanning spectral range was between 4,000 and 400 cm^{-1}. Dried chitosan powder was extensively mixed with KBr pellets before being pressed into an ultra-thin homogeneous disc with 0.5 mm thickness. The chitosan concentration in the samples was estimated to be 2% relative to KBr (El-Naggar et al., 2019).

2.4.2. Raman spectra

Raman characterization of chitosan was classified into three classes, namely index, identification, and morphology classes. The composition class was done by Raman spectroscopy Lab. RAM-HR Evolution Horiba Co, Ontario, Canada. The 532 nm He-Cd edge laser line with grating 1800 (450–850 nm). ND filter 3.2% was used to avoid sample burning employing 10 sec acquisition time, 5 accumulations without delay time, and spike filter (Youssef et al., 2021).

2.4.3. Atomic force microscopy

The surface morphology of the fabricated membranes was examined using a scanning electron microscope (FEG SEM, Philips XL30, 30 kV). Until imaging, the membranes were sputtered with gold. Slitting the membrane sample in liquid nitrogen yielded cross-section samples. The atomic force microscope was used to visualize the quantitative surface topography of RO membranes. (AFM, Brukerdigital instrument, Veeco) in tapping mode for a sampling area of 5 5 m. The Scanning Probe Image Processor (SPIP) 6.7.3 program measured rough analyses using ISO 4287 for a 4 mm cross-section evaluation length. ISO 16,610 used a Gaussian L-Filtering of 2.0 m to remove long wavelengths from the signal. The hydrophilicity of the membrane was manually measured three times by calculating the contact angle between the two surfaces (Hamdy and Taher, 2020).

2.4.4. Antioxidant determination assay

DPPH Radical Scavenging Assay: The radical-scavenging activity of 1,1-diphenyl-2-picrylhydrazyl (DPPH) radical-scavenging activity of chitosan at a concentration of 1 mg mL) was determined according to (Xing et al., 2005). The samples were combined with 375 μL of 99.5% ethanol and 125 μL of 0.02 percent DPPH in 99.5 percent ethanol after being dissolved in 500 μL of distilled water (1 mg mL). After 30 min of incubation in the dark at room temperature, the reduction of the DPPH radical was calculated using a UV–visible spectrophotometer at 517 nm. As an antiradical compound reduces DPPH, its absorption band at 517 nm

disappears. Therefore, higher DPPH-free radical scavenging activities were determined at the reaction mixture's lower absorbance.

DPPH radical-scavenging activity was calculated as follows:

Radical scavenging activity

$$= \frac{\text{Absorbance of control - Absorbance of sample}}{\text{Absorbance of control}} \times 100$$

The control was carried out in the same way, but purified water was used instead of the sample. As a positive control, BHA was used, replacing the sample. The test was conducted three times.

3. Results

3.1. Methodology comparison

A new method for extracting high-quality chitosan from P. clarkii was devised to reduce the preparation time and enhance the purity and quality of the final produced chitosan compared to the traditional way. The conventional method consists of 5 steps; Preparation, deproteinization, demineralization, decolorization, and deacetylation (Fig. 1). The new method (Fig. 2) introduced two additional steps; washing the shell powder (step 2) and dialysis purification (step 7). The steps of decolorization and deacetylation were carried out under reflexive condensers to maintain the reaction conditions and constituents as stable as possible. This modification will help avoid the frequent adjustments needed to compensate for the volatile losses during the decolorization step (6 h) and keep NaOH concentration constant at 50% during the deacetylation step (12 h). As a result, the total time consumed by the new methodology was reduced to 66 h instead of 123 h in the traditional one. This reduction is mainly due to the deacetylation step, which lasted for 12 h at 115 °C instead of 72 h at room temperature. Also, the deproteinization and demineralization steps, conducted during 48 h in the old methodology, were reduced to 24 h in the new methodology.

3.2. Physical form of chitosan

Fig. 3 shows the physical forms of chitosan, indicating the color and size of the particles. High molecular weight chitosan, produced by the traditional method, appears in dark white and medium size granules, closely resembling commercial chitosan. This color may be due to using permanganate potassium in bleaching the chitosan. The new method produced P. clarkii chitosan with chiffon color and fine granules. Using organic solvents such as absolute acetone (colorless) in the new method might have contributed to this faint color of the final product.

Degrading the high molecular weight chitosan into Low molecular weight one by HCl treatment resulted in a product with orange color and coarse granules, while transforming the same chitosan into nanoparticle form, led to a product with light orange color and very fine granules. The addition of TPP during the preparation of nanoparticles may stand behind this orange color. In addition, using the reflexive condenser in the new methodology might have kept the pressure and the concentration at constant levels during the reaction and thus prevented the possible caramelization of the carbohydrate component in chitosan, which causes redness of the color of the final product.

3.3. Chitosan physico-chemical characterization

3.3.1. Degree of deacetylation

Compared to commercial chitosan, P. clarkii chitosan extracted from the exoskeleton wastes exhibited the highest deacetylation extent (89%). This value is higher than the commercial (78%) and the high and low molecular weight Shrimp chitosan and the nano-chitosan (80%). It can be concluded that the new method is more efficient in deacetylating chitin. The modification in the chitosan preparation process, such as the washing step and using a reflexive condenser during the deacetylation step and the purification step, have contributed to this high deacetylation degree. Chitosan degree of deacetylation is the most significant parameter influencing their physicochemical, biological, and mechanical properties. Therefore, before using chitosan in any application, it is necessary to consider some reaction conditions to achieve the best results (Fig. 4).

3.3.2. Solubility, viscosity and molecular weight

The viscosity of P. clarkii chitosan was lower than the commercial chitosan and the shrimp chitosan prepared by the traditional method (H). The other shrimp chitosans (L and N) derived from the original (H) also showed lower viscosity values. The observed low viscosity value of the P. clarkii chitosan may be due to the
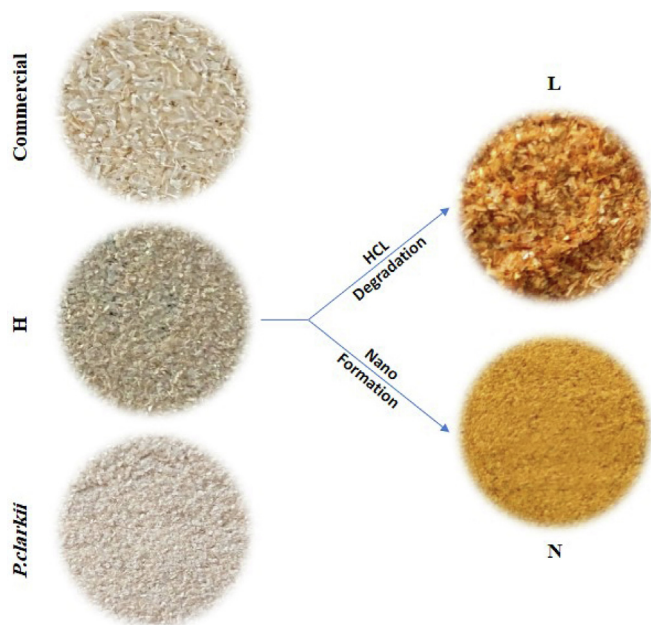

Fig. 3. Photo of chitosan powder for Commercial and P. clarkii chitosan and Shrimp Chitosans High, Low, Nano.
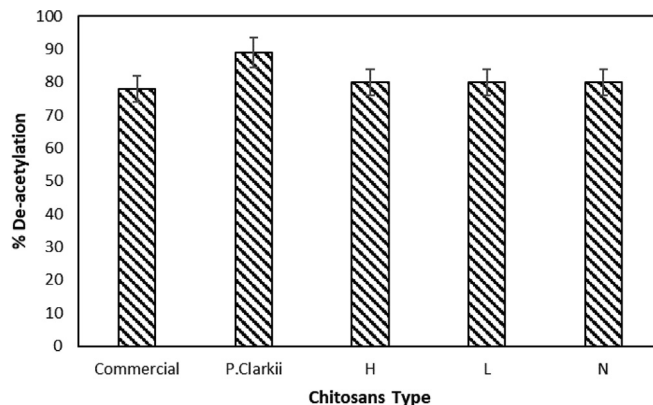

Fig. 4. De-acetylation degree and viscosity index of (H,L&N shrimp chitosan) and (P. clarkii) chitosan.

new methodology, which favored the deacetylation process and stood behind this phenomenon (Fig. 5). The *P. clarkii* chitosan showed the highest solubility compared to other chitosans, i.e., commercial and shrimp chitosans. This enhanced solubility is evidently due to the new preparation conditions, leading to high levels of deacetylation. Depending on the viscosity values, *P. clarkii* chitosan was qualified with a lower molecular weight (200 kDa) than the commercial and the high molecular weight shrimp chitosan (H). The *P. clarkii* chitosan and nano form chitosan showed the lowest molecular weight preparations. The low molecular weight of *P. clarkii* chitosan is about 50% higher than the low molecular weight chitosan but about 60% lower than the commercial and high chitosan. The low molecular weight of *P. clarkii* chitosan makes it more soluble in water than other types of chitosan, achieving 95% solubility.

3.3.3. FTIR spectrum analysis

The data in Fig. 6 presents the FTIR of different Shrimp and *P. clarkii* chitosans. FTIR spectrum of P. clarkii chitosan was not differ-

ent from all other forms of shrimp chitosans (commercial, high, and low molecular weight), except nano-chitosan. Eight bands were detected in the first four forms at 3400, 2900, 2300, 1600, 1400, 1100, 900, and 650 cm^{-1}. These bands are responsible for various functional groups, e.g., alcohol, alkane, alkene, secondary and tertiary amines, amides, phenols, and halo compounds. The strong and wide peak at 3400 represents bonds of both O—H stretching and N—H stretching, while the peaks at 2046.51 cm^{-1}.

3.3.4. Raman spectra

The *P. clarkii* chitosan Raman spectra shown in (Fig. 7), that chitosan was characterized by 13 characteristic; Raman shift peaks at 650, 850, 950, 990, 1055, 1150, 1272, 1423, 1570, 1610, 1920, 2750 and 2930 cm^{-1}. The Peaks at 650 related to OH—, 850 and 1272 cm^{-1} represented vibration of C—H deformation plan where peaks at 1423 represented C—H deformation symmetry and asymmetry, peaks at 1055 and 1150 cm^{-1} are related to C—O stretching, e.g., C—O—C (ring) and C—O—C (ether), respectively. The 1570 cm^{-1} bands represented the vibration of C—N and N—H stretching vibrations, respectively.

3.3.5. Atomic force microscopy (AFM)

The AFM measurements were used to examine the surface of *P. clarkii* chitosan. The three-dimensional AFM images of 5 × 5 nm are shown in (Fig. 8). *P. clarkii* chitosan was measured with an AFM to confirm the form, scale, concentration, and agglomeration predicted by Raman spectra and FTIR spectrum results. The Fig clearly shows that the *P. clarkii* chitosan does not form agglomeration in any specific region. The 3D image showed that the distance between extracted chitosan's highest and deepest points was 728.94 nm. The images obtained revealed homogeneous, smooth surfaces, apparently free of pores and cracks. Preliminary microstructure determinations of films validated this visual assessment using the collected AFM, and the topographic images of the film surface.

3.3.6. Antioxidant assay

The antioxidant activities of aqueous and acetic extracts of chitosans are shown in (Fig. 9). The acetic extract of commercial chitosan increased the scavenging activity by about 20% above water extract. Similar results could be observed with the high molecular weight shrimp chitosan. However, the acetic acid extracts of *P. clarkii* and low molecular weight chitosan and nano-chitosan showed lower antioxidant values than the aqueous extracts. The prepared *P. clarkii* chitosan highly excels these values, probably due to the new preparation methodology keeping the original structure of chitosan in good quality and high purity.

4. Discussion

Agricultural and marine wastes negatively affect the environment and health; however, they are rich in bioactive compounds with antioxidant (Saad et al., 2020a; El-Saadony et al., 2020a; Abdel-Moneim et al., 2022) and antimicrobial activity (Alagawany et al., 2021a). They are used as food additives for preserving juices (Saad et al., 2021b; El-Saadony et al., 2021c), meat (Saad et al., 2020b; Saad et al., 2021c; El-Saadony et al., 2021a), bakery (Saad et al., 2015), and dairy (El-Saadony et al., 2021b). Additionally, feed additives (Alagawany et al., 2021b). Among these compounds is chitosan, which considers a powerful antioxidant and antimicrobial (Abd El-Hack et al., 2020), presenting a large percentage of crustacean wastes.

P. clarkii waste is one of the most severe issues, posing significant environmental and health risks. The purpose of this study was to convert waste P. clarkii into a natural material with a great economic return, e.g., as antibacterial, antifungal agents, and as a
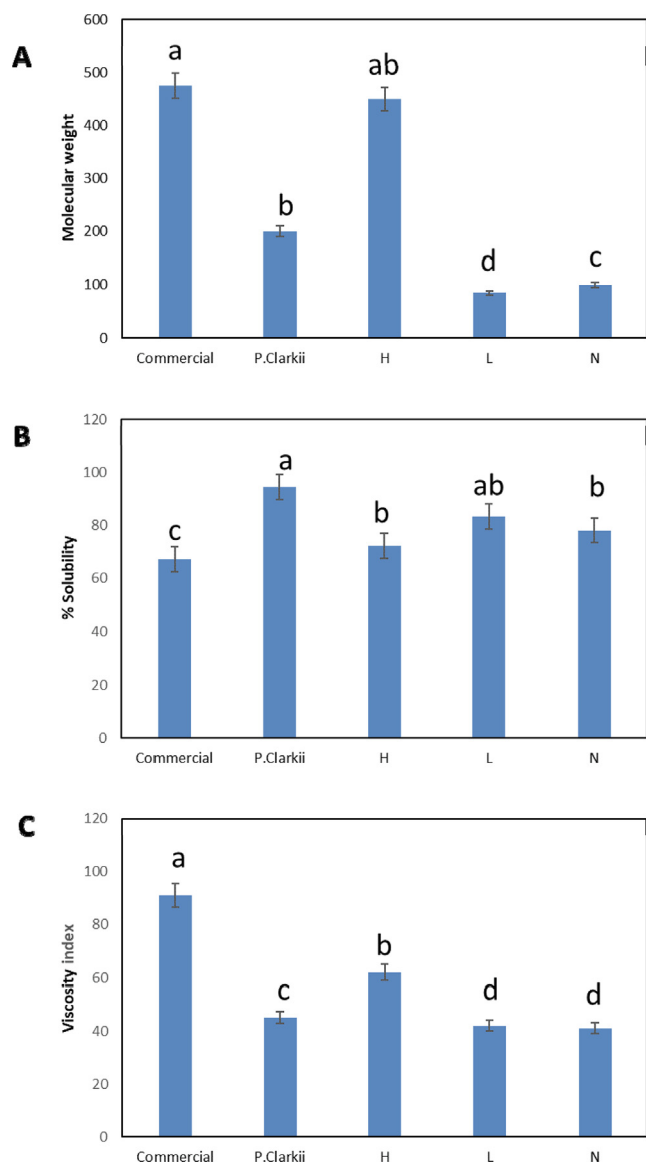

Fig. 5. Solubility, molecular weight and viscosity of (Commercial, H, L&N shrimp chitosan) and (*P. clarkii*) chitosan.
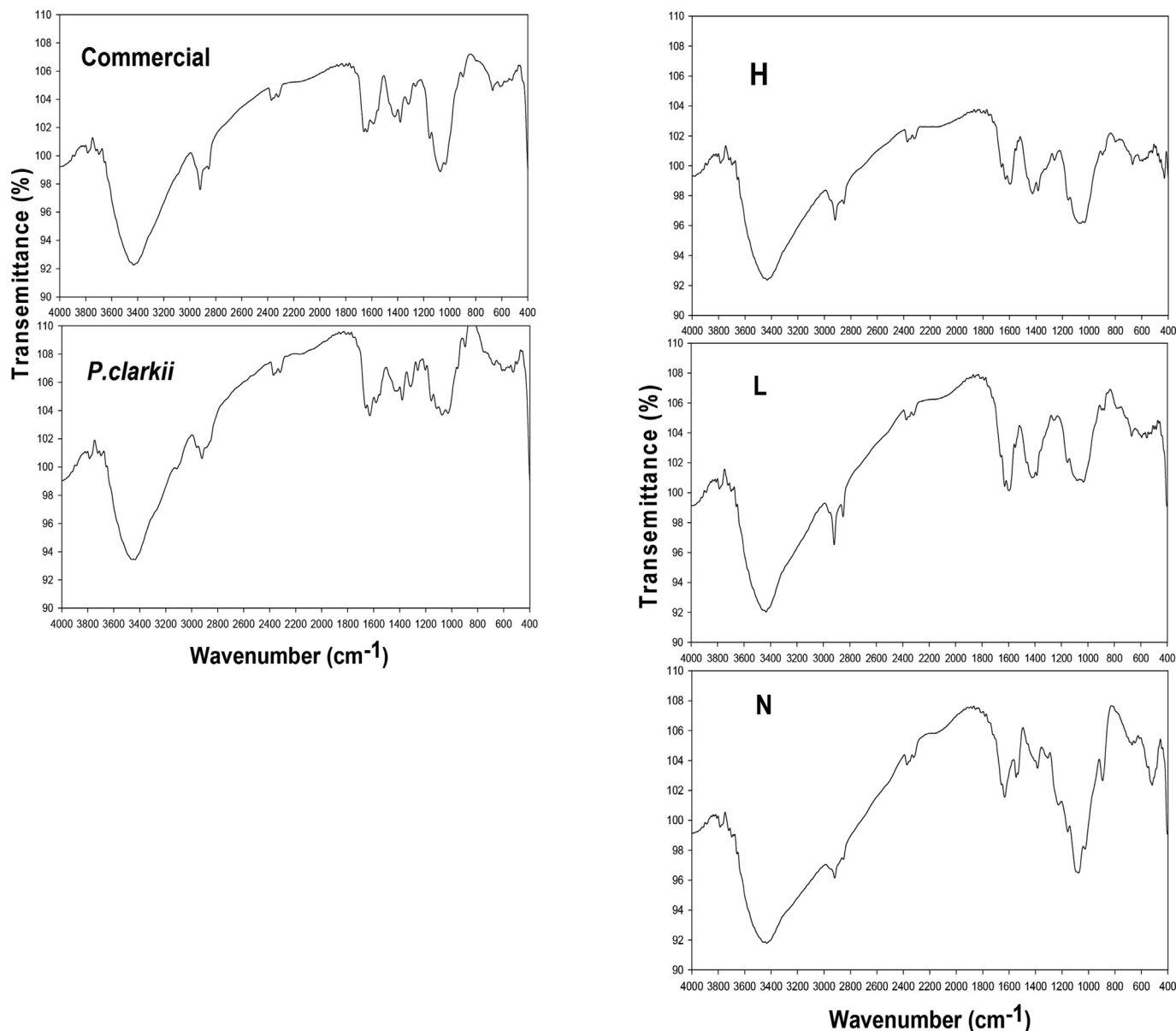
Fig. 6. FTIR of Commercial Shrimp chitosan, *P. clarkii* chitosan, High (H), Low (L) and Nano (N) shrimp chitosans.
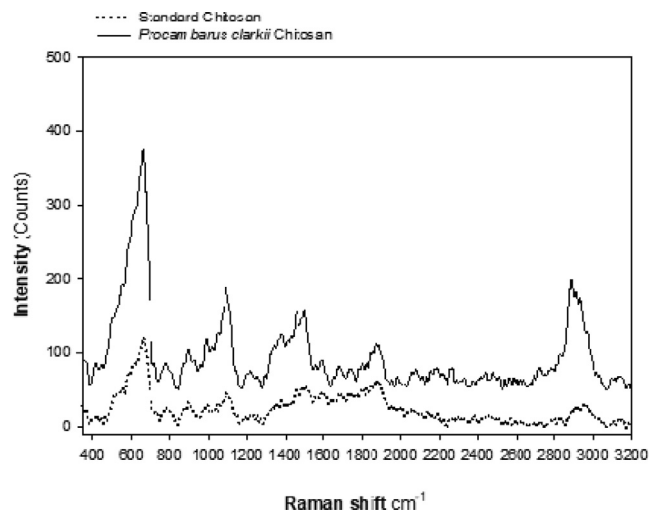

Fig. 7. Raman spectra of Standard chitosan and (*P. clarkii*) chitosan.

helpful material in various agricultural fields (Jin et al., 2019). The extraction method of chitosan determines its molecular weight and chemo-physical properties. Martín-López et al. (2020) found that shrimp chitosan recovered by ultrasound-assisted extraction has a molecular weight of 390 kDa and a water solubility equivalent to 94%. *P. clarkii* chitosan contains various functional groups than commercial and similar to nano and low chitosan. The result of FTIR of *P. clarkii* chitosan revealed different functional groups of organic compounds such as out-of-plane bending (564 cm^{-1}), C—O—C stretching (711 cm^{-1}), and CH2 stretching (1174 cm^{-1}) in chitosan. The most characteristic Raman shift peaks of the P. clarkii chitosan sheet are located between 2750 and 2930 cm^{-1} and related to (C-H), (CH2), and (CH3), confirming its identity in accordance with (Varma and Vasudevan, 2020; Youssef et al., 2021). On the other hand, Fernández-Pan et al. (2010) reported two commercial chitosan samples from cold-water shrimp shells having high degrees of deacetylation (96 and 100%). This indicates that the prepared *P. clarkii* chitosan has a high degree of purity and structural regularity. The aqueous extract of low chitosan exhibited
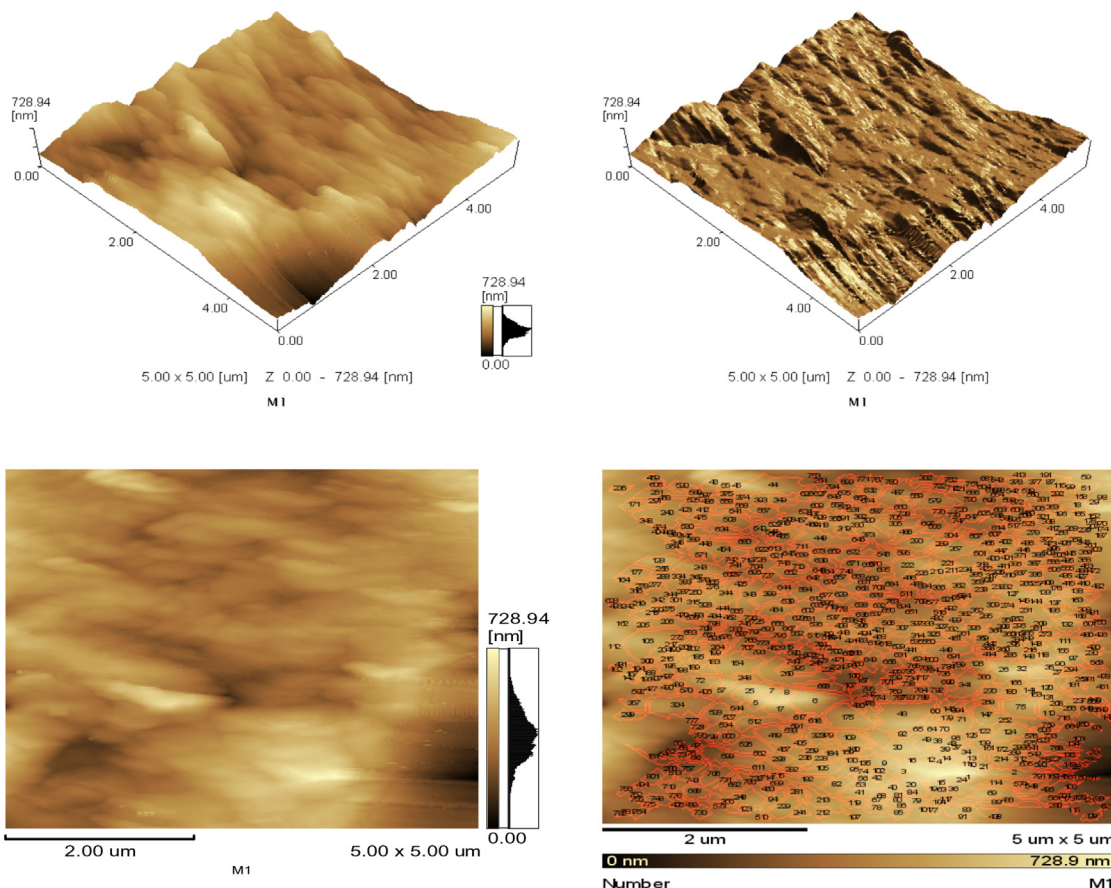
Fig. 8. Three-dimensional atomic force microscopy (AFM) images, cross-section and population of heights in the AFM images of the P. clarkia chitosan.
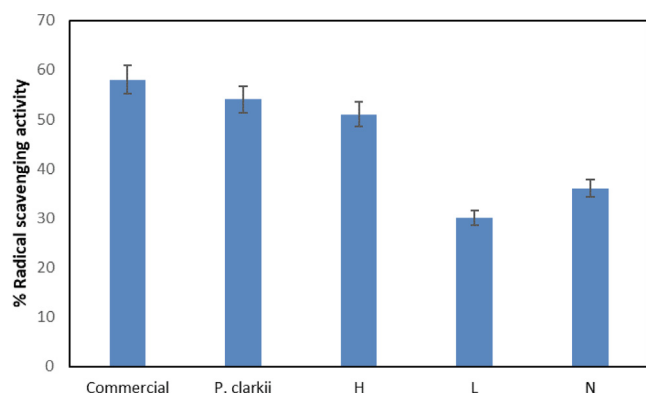

Fig. 9. Antioxidant Activity of Low, High, Nano, Commercial and *P. clarkii* chitosan in (Acetic acid 1% & Water).

the highest antioxidant activity, i.e., 70% followed by *P. clarkii* chitosan with about 60% compared to 75% in cucumber pomace extract (Saad et al., 2021a). The considerable antioxidant activity of P. clarkii qualifies it to be incorporated in functional food to reduce food lipid oxidation (Kabanov and Novinyuk, 2020). Hafsa et al. (2016) found that antioxidant activity of chitin (CHI), classical deacetylated chitosan (CDC), and ultrasound-assisted deacetylated chitosan (UDC) ranged from 4.71 – 21.25%, 11.45–32.78% and 18.27–44.17%, respectively.

The utilizing of chitosan can be maximized by converting to nano form by using the biological pathways, i.e., plant extract (Saad et al., 2021d) and microbial synthesis of nanomaterials i.e., bacteria (Reda et al., 2020; Reda et al., 2021; El-Saadony et al., 2020b; Abd El-Hack et al., 2021; El-Saadony et al., 2022) and fungi (El-Saadony et al., 2021e; El-Saadony et al., 2021f). These pathways produce eco-friendly and cost-effective nanomaterials of small sizes with valuable biological activity (Sheiha et al., 2020; El-Saadony et al., 2021g; El-Saadony et al., 2021h; El-Saadony et al., 2021i). Therefore, the amount of chitosan is reduced and maximized.

5. Conclusion

The new methodology has succeeded in extracting chitosan from P. clarkii in good quality and high purity. It could achieve 89% deacetylation, high solubility, high purity, and medium molecular weight. FTIR, Raman, and Atomic force microscope have confirmed the identity of the P. clarkii chitosan as prepared by a new method. The prepared chitosan has high solubility, low viscosity, and high antioxidant activity, qualifying for different food applications.

Declaration of Competing Interest

The authors declare that they have no known competing financial interests or personal relationships that could have appeared to influence the work reported in this paper.

Acknowledgements

References

Abd El-Hack, M.E., Alaidaroos, B.A., Farsi, R.M., Abou-Kassem, D.E., El-Saadony, M.T., Saad, A.M., Shafi, M.E., Albaqami, N.M., Taha, A.E., Ashour, E.A., 2021. Impacts of supplementing broiler diets with biological curcumin, zinc nanoparticles and *Bacillus licheniformis* on growth, carcass traits, blood indices, meat quality and cecal microbial load. Animals 11 (7), 1878. https://doi.org/10.3390/ani11071878.

Abd El-Hack, M.E., El-Saadony, M.T., Shafi, M.E., Zabermawi, N.M., Arif, M., Batiha, G. E., Khafaga, A.F., Abd El-Hakim, Y.M., Al-Sagheer, A.A., 2020. Antimicrobial and antioxidant properties of chitosan and its derivatives and their applications: A review. Int. J. Biol. Macromol. 1 (164), 2726–2744.

Abdelbacki, A.M., Taha, S.H., Sitohy, M.Z., Abdel-Hamid, M., Rezk, A.A., 2010. Inhibition of tomato yellow leaf curl virus (TYLCV) using whey proteins. Virology Journal, 7, 26.

Abdel-Moneim, A.M.E., El-Saadony, M.T., Shehata, A.M., Saad, A.M., Aldhumri, S.A., Ouda, S.M., Mesalam, N.M., 2022. Antioxidant and antimicrobial activities of *Spirulina platensis* extracts and biogenic selenium nanoparticles against selected pathogenic bacteria and fungi. Saudi J. Biol. Sci. 29 (2), 1197–1209.

Abdel-Shafi, S., Osman, A., Enan, G., El-Nemer, M., Sitohy, M., 2016. Antibacterial activity of methylated egg white proteins against pathogenic G+ and G− bacteria matching antibiotics. Springer Plus 5 (1), 983.

Alagawany, M., El-Saadony, M.T., Elnesr, S.S., Farahat, M., Attia, G., Madkour, M., Reda, F.M., 2021a. Use of lemongrass essential oil as a feed additive in quail's nutrition: its effect on growth, carcass, blood biochemistry, antioxidant and immunological indices, digestive enzymes and intestinal microbiota. Poult. Sci. 100 (6), 101172. https://doi.org/10.1016/j.psj.2021.101172.

Alagawany, M., Madkour, M., El-Saadony, M.T., Reda, F.M., 2021b. Paenibacillus polymyxa (LM31) as a new feed additive: Antioxidant and antimicrobial activity and its effects on growth, blood biochemistry, and intestinal bacterial populations of growing Japanese quail. Anim. Feed Sci. Technol. 276, 114920. https://doi.org/10.1016/j.anifeedsci.2021.114920.

Aranaz, I., Mengibar, M., Harris, R., Panos, I., Miralles, B., Acosta, N., Galed, G., Heras, A., 2009. Functional characterization of chitin and chitosan. Curr. Chem. Biol. 3 (2), 203–230.

Chobert, J.M., Sitohy, M., Billaudel, S., Dalgalarrondo, M., Haertlé, T., 2007. Anticytomegaloviral activity of esterified milk proteins and L-polylysines. Journal of Molecular Microbiology and Biotechnology 13 (4), 255–258.

Czechowska-Biskup, R., Wach, R.A., Rosiak, J.M., Ulański, P., 2018. Procedure for determination of the molecular weight of chitosan by viscometry. Prog. Chem. Appl. Chitin. Deriv. XXIII, 45–54.

Divya, K., Rebello, S., Jisha, M., 2014. A simple and effective method for extraction of high purity chitosan from shrimp shell waste, Proc. of the Intl. Conf. on Advances In Applied Science and Environmental Engineering —ASEE 2014.

El-Naggar, M., Salaah, S., El-Shabaka, H., El-Rahman, F.A., Khalil, M., Suloma, A., 2021. Efficacy of dietary chitosan and chitosan nanoparticles supplementation on health status of Nile tilapia, Oreochromis niloticus (L.). Aquac. Rep. 19, 100628. https://doi.org/10.1016/j.aqrep.2021.100628.

El-Naggar, M.M., Abou-Elmagd, W.S.I., Suloma, A., El-Shabaka, H.A., Khalil, M.T., Abd El-Rahman, F.A., 2019. Optimization and physicochemical characterization of chitosan and chitosan nanoparticles extracted from the crayfish *Procambarus clarkii* wastes. J. Shellfish Res. 38 (2), 385. https://doi.org/10.2983/035.038.022010.2983/035.038.0220.s1.

El-Saadony, M.T., Abd El-Hack, M.E., Swelum, A.A., Al-Sultan, S.I., El-Ghareeb, W.R., Hussein, E.O.S., Ba-Awadh, H.A., Akl, B.A., Nader, M.M., 2021a. Enhancing quality and safety of raw buffalo meat using the bioactive peptides of pea and red kidney bean under refrigeration conditions. Ital. J. Anim. Sci. 20 (1), 762–776.

El-Saadony, M.T., ALmoshadak, A.S., Shafi, M.E., Albaqami, N.M., Saad, A.M., El-Tahan, A.M., et al., 2021i. Vital roles of sustainable nano-fertilizers in improving plant quality and quantity-an updated review. Saudi J. Biol. Sci. 28 (12), 7349–7359.

El-Saadony, M.T., Elsadek, M.F., Mohamed, A.S., Taha, A.E., Ahmed, B.M., Saad, A.M., 2020a. Effects of chemical and natural additives on cucumber juice's quality, shelf life, and safety. Foods 9 (5), 639.

El-Saadony, M.T., Khalil, O.S., Osman, A., Alshilawi, M.S., Taha, A.E., Aboelenin, S.M., Shukry, M., Saad, A.M., 2021. Bioactive peptides supplemented raw buffalo milk: Biological activity, shelf life and quality properties during cold preservation. Saudi J. Biol. Sci. 28 (8), 4581–4591.

El-Saadony, M.T., Saad, A.M., El-Akkad, H.A., El-Tahan, A.M., Alshahrani, O.A., Alshilawi, M.S., Ahmed, A.I., 2022. Flavoring and extending the shelf life of cucumber juice with aroma compounds-rich herbal extracts at 4° C through controlling chemical and microbial fluctuations. Saudi J. Biol. Sci. 29 (1), 346–354.

El-Saadony, M. T., Saad, A. M., Taha, T. F., Najjar, A. A., Zabermawi, N. M., Nader, M. M., et al., 2021e. Selenium nanoparticles, from Lactobacillus paracasei HM1

capable of antagonizing animal pathogenic fungi, as a new source from human breast milk. Saudi J. Biol. Sci. 28 (12), 6782–6794.

El-Saadony, M.T., Alkhatib, F.M., Alzahrani, S.O., Shafi, M.E., El. Abdel-Hamid, S., Taha, T.F., Aboelenin, S.M., Soliman, M.M., Ahmed, N.H., 2021f. Impact of mycogenic zinc nanoparticles on performance, behavior, immune response, and microbial load in Oreochromis niloticus. Saudi J. Biol. Sci. 28 (8), 4592–4604.

El-Saadony, M.T., Desoky, E.-S., Saad, A.M., Eid, R.S.M., Selem, E., Elrys, A.S., 2021g. Biological silicon nanoparticles improve Phaseolus vulgaris L. yield and minimize its contaminant contents on a heavy metals-contaminated saline soil. J. Environ. Sci. 106, 1–14.

El-Saadony, M.T., El-Hack, A., Mohamed, E., Taha, A.E., Fouda, M.M., Ajarem, J.S., N Maodaa, S., Allam, A.A., Elshaer, N., 2020b. Ecofriendly synthesis and insecticidal application of copper nanoparticles against the storage pest Tribolium castaneum. Nanomaterials 10, 587.

El-Saadony, M.T., Saad, A.M., Najjar, A.A., Alzahrani, S.O., Alkhatib, F.M., Shafi, M.E., Selem, E., Desoky, E.-S.-M., Fouda, S.-E.-S.-E.-S., El-Tahan, A.M., 2021h. The use of biological selenium nanoparticles in controlling Triticum aestivum L. crown root and rot diseases induced by Fusarium species and improve yield under drought and heat stress. Saudi J. Biol. Sci. 28 (8), 4461–4471.

El-Saadony, M.T., Sitohy, M.Z., Ramadan, M.F., Saad, A.M., 2021i. Green nanotechnology for preserving and enriching yogurt with biologically available iron (II). Innov. Food Sci. Emerg. Technol. 69, 102645. https://doi.org/10.1016/j.ifset.2021.102645.

Fernández-Pan, I., Ziani, K., Pedroza-Islas, R., Maté, J., 2010. Effect of drying conditions on the mechanical and barrier properties of films based on chitosan. Dry. Technol. 28, 1350-1358.

Hafsa, J., Smach, M.A., Charfeddine, B., Limem, K., Majdoub, H., Rouatbi, S., 2016. Antioxidant and antimicrobial proprieties of chitin and chitosan extracted from Parapenaeus Longirostris shrimp shell waste. Ann. Pharm. Fr. Elsevier 74 (1), 27–33.

Hamdy, G., Taher, A., 2020. Enhanced chlorine-resistant and low biofouling reverse osmosis polyimide-graphene oxide thin film nanocomposite membranes for water desalination. Polym. Eng. Sci. 60 (10), 2567–2580.

Ibrahim, A., Khalil, M., 2009. The red swamp crayfish in Egypt (a fast spreading freshwater invasive crustacean). J. Egypt. Acad. Soc. Environ. Develop. Cairo, Egypt.

Jin, S., Jacquin, L., Xiong, M., Li, R., Lek, S., Li, W., Zhang, T. 2019. Reproductive pattern and population dynamics of commercial red swamp crayfish (Procambarus clarkii) from China: implications for sustainable aquaculture management. PeerJ, 7, e6214.

Kabanov, V.L., Novinyuk, L.V., 2020. Chitosan application in food technology: A review of rescent advances. Agroecol. Sustain. Food 3, 10-15.

Kasaai, M.R., Arul, J., Charlet, G., 2013. Fragmentation of chitosan by acids. Sci. World J. 2013.

Kumar, M.N.R., 2000. A review of chitin and chitosan applications. React. Funct. Polym. 46, 1-27.

Liu, H., Gao, C., 2009. Preparation and properties of ionically cross-linked chitosan nanoparticles. Polym. Adv. Technol. 20, 613-619.

Martín-López, H., Pech-Cohuo, S.C., Herrera-Pool, E., Medina-Torres, N., Cuevas-Bernardino, J.C., Ayora-Talavera, T., Espinosa-Andrews, H., Ramos-Díaz, A., Trombotto, S., Pacheco, N., 2020. Structural and Physicochemical Characterization of Chitosan Obtained by UAE and its Effect on the Growth Inhibition of Pythium ultimum. Agriculture 10, 464.

No, H.K., Meyers, S.P., 1989. Crawfish chitosan as a coagulant in recovery of organic compounds from seafood processing streams. J. Agric. Food Chem. 37, 580-583.

Osman, A., El-Didamony, G., Sitohy, M., Khalifa, M., Enan, G., 2016. Soybean glycinin basic subunit inhibits methicillin resistant-vancomycin intermediate Staphylococcus aureus (MRSA-VISA) in vitro. International Journal of Applied Research in Natural Products 9 (2), 17–26.

Peniche, C., Argüelles-Monal, W., 2001. Chitosan based polyelectrolyte complexes, Macromolecular Symposia. Macromol. Symp. pp. 103-116.

Pillai, C.K.S., Paul, W., Sharma, C.P., 2009. Chitin and chitosan polymers: Chemistry, solubility and fiber formation. Prog. Polym. Sci. 34 (7), 641–678.

Puvvada, Y.S., Vankayalapati, S., Sukhavasi, S., 2012. Extraction of chitin from chitosan from exoskeleton of shrimp for application in the pharmaceutical industry. Int. curr. pharm. 1, 258-263.

Reda, F.M., El-Saadony, M.T., Elnesr, S.S., Alagawany, M., Tufarelli, V., 2020. Effect of dietary supplementation of biological curcumin nanoparticles on growth and carcass traits, antioxidant status, immunity and caecal microbiota of Japanese quails. Animals 10 (5), 754.

Reda, F.M., El-Saadony, M.T., El-Rayes, T.K., Attia, A.I., El-Sayed, S.A., Ahmed, S.Y., Madkour, M., Alagawany, M., 2021. Use of biological nano zinc as a feed additive in quail nutrition: biosynthesis, antimicrobial activity and its effect on growth, feed utilisation, blood metabolites and intestinal microbiota. Ital. J. Anim. Sci. 20 (1), 324–335.

Saad, A.M., Elmassry, R.A., Wahdan, K.M., Ramadan, F.M., 2015. Chickpea (Cicer arietinum) steep liquor as a leavening agent: effect on dough rheology and sensory properties of bread. Acta Period. Technol. (46), 91–102 https://doi.org/10.2298/APT1546091S.

Saad, A.M., El-Saadony, M.T., Mohamed, A.S., Ahmed, A.I., Sitohy, M.Z., 2021. Impact of cucumber pomace fortification on the nutritional, sensorial and technological quality of soft wheat flour-based noodles. Int. J. Food Sci. 56 (7), 3255–3268.

Saad, A.M., Mohamed, A.S., El-Saadony, M.T., Sitohy, M.Z., 2021b. Palatable functional cucumber juices supplemented with polyphenols-rich herbal extracts. LWT - Food Sci. Technol. 148, 111668. https://doi.org/10.1016/j.lwt.2021.111668.

Saad, A.M., Mohamed, A.S., Ramadan, M.F., 2020a. Storage and heat processing affect flavors of cucumber juice enriched with plant extracts. Int. J. Veg. Sci., 1–11

Saad, A.M., Osman, A.O.M., Mohamed, A.S., Ramadan, M.F., 2020b. Enzymatic hydrolysis of Phaseolus vulgaris protein isolate: Characterization of hydrolysates and effect on the quality of minced beef during cold storage. Int. J. Pept. Res. Ther. 26 (1), 567–577.

Saad, A.M., Sitohy, M.Z., Ahmed, A.I., Rabie, N.A., Amin, S.A., Aboelenin, S.M., Soliman, M.M., El-Saadony, M.T., 2021c. Biochemical and functional characterization of kidney bean protein alcalase-hydrolysates and their preservative action on stored chicken meat. Molecules 26 (15), 4690. https://doi.org/10.3390/molecules26154690.

Saad, A.M., El-Saadony, M.T., El-Tahan, A.M., Sayed, S., Moustafa, M.A., Taha, A.E., Taha, T.F., Ramadan, M.M., 2021d. Polyphenolic extracts from pomegranate and watermelon wastes as substrate to fabricate sustainable silver nanoparticles with larvicidal effect against Spodoptera littoralis. Saudi J. Biol. Sci. 28 (10), 5674–5683.

Shard, P., Sharma, D., Bhatia, A., 2014. Optimization and effects of physico-chemical parameters on synthesis of chitosan nanoparticles by ionic gelation technique. Int. J. Drug Deliv. 6, 58.

Sheiha, A.M., Abdelnour, S.A., El-Hack, A., Mohamed, E., Khafaga, A.F., Metwally, K.A., El-Saadony, M.T., 2020. Effects of dietary biological or chemical-synthesized nano-selenium supplementation on growing rabbits exposed to thermal stress. Animals 10 (3), 430.

Simpson, B., Gagne, N., Simpson, M., 1994. Bioprocessing of chitin and chitosan. In: Fisheries Processing. Springer, pp. 155–173.

Sitohy, M., Chobert, J.-M., Karwowska, U., Gozdzicka-Jozefiak, A., Haertlé, T., 2006. Inhibition of bacteriophage M13 replication with esterified milk proteins. J. Agric. Food Chem. 54 (11), 3800–3806.

Sitohy, M., Mahgoub, S., Osman, A., 2011. Controlling psychrotrophic bacteria in raw buffalo milk preserved at 4 °C with esterified legume proteins. Food Sci. Technol. 44 (8), 1697–1702.

Sitohy, M., Mahgoub, S., Osman, A., El-Masry, R., Al-Gaby, A., 2013. Extent and Mode of Action of Cationic Legume Proteins against Listeria monocytogenes and Salmonella Enteritidis. Probiotics Antimicrob. Proteins 5 (3), 195–205.

Sitohy MZ, Mahgoub SA, Osman AO 2012. In vitro and in situ antimicrobial action and mechanism of glycinin and its basic subunit. Int. J. Food Microbiol. 154(1-2), 19–29.

Sitohy, M., Billaudel, S., Haertlé, T., Chobert, J.-M. 2007 Antiviral activity of esterified α-lactalbumin and β-lactoglobulin against herpes simplex virus type 1. Comparison with the effect of acyclovir and L-polylysines. J. Agric. Food Chem. 55(25), pp. 10214–10220.

Sitohy, M., Osman, A., El-Deeb, S., Farag, G.K., Tolba, H.M.N., 2021b. 2021b H5N1 Avian Flu Infection in Hubbard Broiler Chicken Can Be Prevented or Cured by Methylated Soy Protein During 42 Days Rearing. Probiotics Antimicrob. Proteins 10, 1–5.

Sitohy, M., Taha, S., Abdel-Hamid, M., Hamed, A., Osman, A., 2021a. Protecting potato plants against PVX and PVY viral infections by the application of native and chemically modified legume proteins. J. Plant Dis. Prot. 128 (4), 1101–1114.

Sitohy, M., Taha, S., Osman, A., et al., 2020 Antiviral action of native and methylated lactoferrin and β-lactoglobulin against potato virus Y (PVY) infected into potato plants grown in an open field. Antibiotics 9(7), pp. 1–13, 430

Swelum, A.A., Shafi, M.E., Albaqami, N.M., El-Saadony, M.T., Elsify, A., Abdo, M., Taha, A.E., Abdel-Moneim, A-M., Al-Gabri, N.A., Almaiman, A.A., Al-wajeeh, A.S., Tufarelli, V., Staffa, V.N., Abd El-Hack, M.E., 2020. COVID-19 in Human, Animal, and Environment: A Review. Front. Vet. Sci. 7, 578.

Taha, S.H., Mehrez, M.A., Sitohy, M.Z., Abdel-Hamid, M., Kilany, W.H., 2010. Effectiveness of esterified whey proteins fractions against Egyptian Lethal Avian Influenza A (H5N1). Virol. J. 7, 330.

Varma, R., Vasudevan, S., 2020. Extraction, Characterization, and Antimicrobial Activity of Chitosan from Horse Mussel Modiolus modiolus. ACS Omega 5, 20224–20230.

Xing, R., Yu, H., Liu, S., Zhang, W., Zhang, Q., Li, Z., Li, P., 2005. Antioxidant activity of differently regioselective chitosan sulfates in vitro. Bioorg. Med. Chem. 13, 1387–1392.

Youssef, F., Mohamed, G., Ismail, S., Elzorba, H., Galal, A., Elbanna, H., 2021. Synthesis, Characterization and In vitro Antimicrobial Activity of Florfenicol-Chitosan Nanocomposite. Egypt. J. Chem. 64, 941–948.

Zhao, D., Yu, S., Sun, B., Gao, S., Guo, S., Zhao, K., 2018. Biomedical applications of chitosan and its derivative nanoparticles. Polymers 10, 462.